CHAPTER 195

FLUSHING BEHAVIOUR OF A COASTAL MARINA

R. A. Schwartz [*] and J. Imberger [**]

Abstract

The flushing characteristics of a newly constructed marina were determined from a comprehensive field study which included a dye dilution experiment together with measurements of barotropic and baroclinic forcing parameters. The results to be presented show that the major exchange process in this particular marina is a baroclinic circulation, and that the exchange rate is controlled by the harbour entrance geometry.

1.0 Introduction

The continued growth of population centres along the Western Australian coast implies that the existing recreational and commercial boating facilities will not satisfy future demand. To increase the number of sheltered boat moorings, state and local authorities are constructing new marinas and enlarging the existing facilities. State regulations require that such projects be preceded by an Environmental Review and Management Planning (E.R.M.P.) report, wherein the potential impact on water quality must be assessed. Since the quality of the water in a coastal harbour largely depends on the natural ability of the harbour to flush out trapped pollutants, any water quality forecast requires an understanding of how the water is exchanged with the adjoining sea.

The circulation of water between a marine harbour and the connecting sea is generally the result of natural parameters such as the local tidal range, wave climate, meteorological conditions, and water density differences. Depending on the geographical location, one or more of these variables can dominate the exchange properties of a harbour. Pollutants such as pesticides, heavy metals, and organic compounds enter a marina basin via surface run-off, leaching from boats' anti-fouling paint, and spillages from service facilities located within the marina boundaries. If pollutant concentrations are allowed to increase above critical levels, then the result is sub-standard water quality as characterized by a reduction in dissolved oxygen and the presence of algal blooms. Detrimental water quality within a marine harbour can be avoided by reducing the potential sources of pollutants,

* Graduate student, Department of Civil Engineering,
   University of Western Australia, Nedlands, W.A., 6009, Australia.
** Professor of Civil Engineering, and Director of the Centre for Water Research,
   University of Western Australia, Nedlands, W.A., 6009, Australia.

and by maintaining an optimal flushing rate. The water exchange rate is affected by factors such as the planform geometry, entrance dimensions and number of entrances (Nece, 1984). So, once the geometrical effects and locally dominant flushing parameters are understood, a marina can be designed to have an optimal water exchange rate.

To understand the flushing characteristics of a marine harbour situated on the Western Australian coastline, the Centre for Water Research (CWR) in conjuction with the State Department of Marine and Harbours conducted a series of field experiments in a newly constructed marina. The specific aims of this project were to quantify the flushing rate as a function of time and space, identify the dominant flushing mechanisms, and measure fine-scale dissipation rates of turbulent kinetic energy. The results will be used to develop a strategy for water quality monitoring in all marinas under the control of the Department of Marine and Harbours and aid in designing future marinas.

The marina chosen for the field experiments is known as Hillarys Boat Harbour. It is located on the southwest Australian coast approximately 26 km north of Fremantle. The tidally averaged depth of Hillarys Boat Harbour is approximately 5.5 m. With a water surface area of about 2.46×10^5 m^2, its tidally averaged volume can be estimated as 1.3×10^6 m^3. The harbour was designed to contain 1,000 boat moorings. It has a single asymmetric entrance which is 90 m wide by 5 m deep, and is oriented to the north as shown in Figure 1.
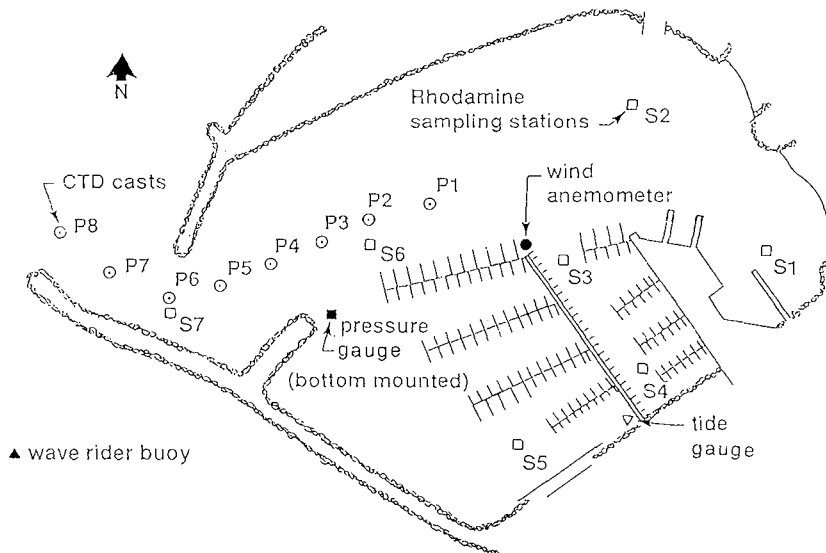
Figure 1 Hillarys Boat Harbour planform together and sampling sites.

The flushing time of Hillarys Boat Harbour was determined by uniformly seeding the harbour with a fluorescent dye and subsequently monitoring its dilution as a function of time and space. Simultaneous to the dye dilution experiment, vertical profiles of salinity and temperature were measured with Conductivity Temperature Depth (CTD) probes, and a microstructure probe was deployed to estimate the dissipation of turbulent kinetic energy. The *Djinnang III* was the largest of the two CWR research vessels used for

collecting data. Its onboard instruments included a CTD probe, a microstructure probe, and a mini-ranger system for establishing the coordinates of the sampling stations. The other research vessel, known as the *Trail Craft,* also had a CTD probe onboard and was outfitted with a fluorometer which measured the concentration of the fluorescent dye. These vessels and their respective instruments were used for three weeks to monitor the response of the water body to natural forcing conditions.

Wind speeds, tidal amplitudes, and wave statistics were measured with remotely operated devices positioned as shown in Figure 1. Wind directions were obtained from the Bureau of Meteorology's weather station at Ocean Reef, located approximately 5 km north of the harbour. A CWR mini-logger was installed to measure wind speeds. The mini-logger was attached to RIMCO® cup anemometer and recorded a sample every ten minutes. Other remote recording instruments were installed and monitored by the Department of Marine and Harbours. These included a float/counter-weight type tide gauge mounted within the marina, a bottom-mounted Weslog® logger for recording wave actions inside the marina, and a Datawell® series 6000 wave-rider buoy located outside the marina.

2.0 Experimental Programme

Early on 29 April 1987 (Julian day 119), 60 litres of a 20% Rhodamine WT aqueous solution were diluted with seawater and injected into the harbour from a small dinghy. The dye mixture was pumped through a diffuser end-pipe which was continuously raised and lowered while the dinghy slowly criss-crossed the interior of the harbour. Immediately following the injection of the dye, a monitoring cycle was initiated at seven interior stations (S1 - S7 shown in Figure 1) to determine the dilution rate of the Rhodamine WT tracer as a function of time and space. At each station, tracer concentrations were measured just below the surface, at mid-depth and 1 m from the bottom. Water was selectively withdrawn through a special disc inlet (Imberger and Berman, 1986) with an effective vertical resolution of 0.30 m, and pumped up to a debubbler mounted one metre above a Turner Designs® model 10 series fluorometer. A gravity outflow from the debubbler supplied the fluorometer with a bubble-free stream of water, which was analysed and recorded on a Multiterm® micro-computer before being discharged overboard. The natural fluorescence of the marina water was measured prior to injecting the dye, and the fluorometer was tuned to zero out this 'blank' concentration. Each station was initially sampled several times a day. However as the experiment progressed, it was only necessary to sample once a day or once every other day.

In conjunction with the dye dilution experiment, free-falling and rising probes were deployed from the *Djinnang III* and the smaller *Trail Craft* to obtain density, salinity and temperature profiles inside and outside of the harbour. The free-falling CTD probe (Fozdar, 1983) consisted of a pressure transducer for determining depth, a SEA-BIRD SBE-3 oceanographic thermometer for temperature measurements and a SEA-BIRD SBE-4 conductivity cell for determining salinities. Water parcels were sampled at 50 Hz as the probe descended to the bottom with a fall-rate of 1 ms^{-1}. This is equivalent to a spatial resolution of 2 cm. The vertically rising microstructure profiler (RMP) (Carter and Imberger, 1986) was used to measure fine-scale temperature gradients from which rates of turbulent kinetic energy dissipation were estimated. As the RMP rises at 0.1 ms^{-1} from a pre-set depth, its pressure transducer, two fast-response thermistors and two specially designed conductivity cells sample at 100 Hz. This results in a spatial resolution of 1 mm, which represents a 200% increase in resolution over the CTD probe.

3.0 Data Analysis

Profiles representing the measured dye concentrations at every sampling station for each circuit showed that a non-uniform dye distribution existed throughout the harbour for 24 hours after the dye was injected. This initial depth and spatial variation is primarily a reflection of the logistics involved in manually seeding such a large volume of water to obtain a uniform distribution. A well-mixed condition was eventually achieved on Julian day 120, one day after the dye was introduced into the system.

<u>Dilution Rate</u>

The rate at which the tracer concentration decreased with time is shown in Figure 2. The plotted data were best described by an exponential curve fit of the form

$$C = 169 \times 10^{(-0.0917\,t)} \tag{1}$$

where C is the concentration value for a particular Julian day value t. Using an initial Rhodamine WT concentration of 1.35×10^{-9} on Julian day 120, an e-folding time was calculated as the time required for the initial concentration to drop to C / e. Solving equation (1) for t yielded a corresponding Julian day value of 125. Thus, the measured dilution rate of Rhodamine WT had an e-folding time of 5 days!

Rhodamine WT is quite stable with respect to photochemical decay, sediment absorption, and pH; however, salinity and temperature can significantly affect the fluorescence of Rhodamine WT. Smart and Laidlaw (1977) reported contradictory results from two independent tests which produced radically different decay rates for the fluorescence of Rhodamine WT with long-term exposure ($\sim$10 days) in saline environments. To evaluate the effect of salinity on the fluorescence of Rhodamine WT in the harbour, a laboratory experiment was conducted under controlled conditions in which samples with dye concentrations of 1×10^{-9} were monitored for two weeks. The results showed a 3% reduction in the initial dye fluorescence for a typical seawater chlorinity of 19 $^o/_{oo}$ (salinity 35 $^o/_{oo}$). The effect of temperature on fluorescence intensity was determined from an empirical equation of the form

$$F = F_0\, e^{-0.027\,t} \tag{2}$$

where F is the fluorescence at a standard temperature, F_0 is the fluorescence at the sample temperature, and t represents the difference between the standard and sample temperatures (^{o}C). The error in fluorescence intensity which can be attributed to temperature variations was estimated to be less than 5%. Because the combined error in fluorescence intensity due to salinity and temperature was less than 8%, it was concluded that the observed dye loss in the harbour was caused by flushing actions and not chemical degradation.

<u>Tidal Motions</u>

The tides of the southwestern Australian coast are unusual because they are generally diurnal with amplitudes so small that astronomical and meteorological forces produce changes in the sea level of the same order of magnitude. Similar characteristics were exhibited in the sea level fluctuations measured during the three week field study, namely, an overriding diurnal pattern with amplitudes less than one metre.

The overall contribution to flushing from the oscillating sea level was determined by using the tidal prism method. This method assumes that the exchange flow is only a function of the tidal range, and any mass removed on the ebb tide does not return on the following flood tide. These assumptions were proven to be valid for Hillarys Boat Harbour by aerial photographs taken on Julian day 119. The photographs showed that wind-induced circulations outside the harbour quickly dispersed any dye which was flushed out with the ebbing tide. Given that the sea level prism is about 0.5 m, an e-folding time for the tidal flushing mechanism was calculated to be 11 tidal cycles. This corresponds to 11 days since the tidal cycle was primarily diurnal. A comparison between the analytical e-folding time of 11 days and the measured e-folding time of 5 days revealed a discrepancy which was too large to be attributed to experimental error. Therefore, the tide was not the dominant mechanism for driving an exchange flow between the harbour and the sea.
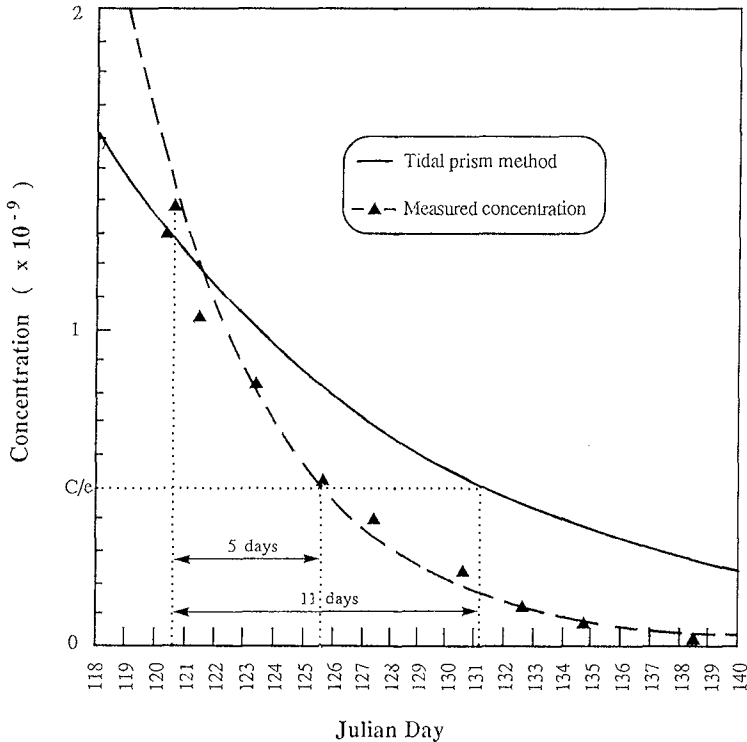
Figure 2 Comparison of the tidal prism method with the measured dilution rate.

Stratification

Hillarys Boat Harbour is situated on the coastal border of an inland freshwater mound which rises 70 m above sea level. Submarine groundwater discharges along the coast in this area were first reported by Johannes (1980). Freshwater patches were detected by the CTD probe near the bottom and along the shoreline inside the marina. The quantity of freshwater discharging into the marina was estimated to be about 2×10^3 m^3 day^{-1}.

Knowledge about the density structure of a water body is useful for quantifying the internal transport processes associated with advection, mixing and diffusion. The CTD and the vertically rising microstructure profiler (RMP) were deployed at various points in the vicinity of the harbour to measure conductivity and temperature characteristics. From these measurements, practical salinities and densities were calculated using the practical salinity scale and equations of state given in UNESCO (1981). The raw data were processed to account for the different response characteristics of the probes' sensors and their vertical separation. In this way, all the data relating to the same parcel of fluid were matched with each other. Failure to properly match the conductivity, temperature and depth signals results in unrealistic spiking in the salinity and density calculations. After the CTD and RMP data were adjusted for vertical separation, a recursive time series technique developed by Fozdar et al. (1985) was used to match the sensor response times.

Data collected from a series of equally spaced CTD drops were used to produce contour plots of salinity, temperature and density profiles. An interesting example of an isopycnal plot is shown in Figure 3. The density structure shown in this figure is indicative of a baroclinic circulation caused by a gravitational adjustment. Only a few of the isopycnal plots revealed such a pattern, while the remainder showed density structures characteristic of well-mixed to longitudinally stratified conditions. Thus, no single steady-state stratification condition existed within the harbour during this study. In Table 1, the various isopycnal plots were classified according to the degree of stratification exhibited along with measured wind speeds and tidal conditions. The noteworthy feature in this table is that an internal frontal structure resembling a standing wave was observed to occur under light wind conditions (less than 3 ms^{-1}) and predominantly on the ebb tide. This observation is supported by Simpson and Nunes (1981), who reported similar frontogenesis behavior occurring on the ebb tide in several different estuaries. Dyer (1973) also described frontal formations in a partially mixed estuary as a consequence of a distinct two-layer flow system.

Wind Effects

Air currents moving across an exposed body of water exert a drag force on the water surface in the form of a shear stress. This mechanism generates surface waves which act to transfer momentum and mechanical energy from the wind to the water surface, thereby contributing to the circulation dynamics of the water body. Effects such as topographic gyres, differential deepening of the mixed-layer and subsequent gravitational adjustments are all directly related to the input energy flux from the wind.

Imberger (1985) defined the surface mixed-layer in a stratified water body as that part of the water column which is directly influenced by the momentum and turbulence introduced by a surface wind stress. Production of turbulent kinetic energy (TKE) at the base and surface of the mixed-layer causes the mixed-layer depth to fluctuate. TKE produced at the base of the mixed-layer is known as "shear production" and is primarily caused by seiching motions. At the surface, TKE production is commonly referred to as "stirring". As the wind-induced TKE is dissipated down through the water column by viscous forces, heavier water from below the mixed-layer is entrained. The result is that the mixed-layer deepens, the potential energy of the water column increases, and a longitudinal density gradient is established. A subsequent reduction in TKE allows the density structure to "relax", thereby creating a gravitational current which further redistributes the mass within the water body.

Table 1 Classification of density contour plots.

Julian day	Time	Stratification	Wind Speed (ms-1)	Tide
119A	11:20 - 11:27	V.S.	< 3	Ebb
119B	13:12 - 13:27	V.S.	< 3	Ebb
119C	16:24 - 16:45	F	< 3	Ebb
119D	18:03 - 18:12	F	< 3	Ebb
119E	18:53 - 19:07	F	< 3	Ebb
120A	08:12 - 08:56	M	8	Flood
120B	12:44 - 12:59	M	10	Ebb
120C	14:28 - 14:59	M	12	Ebb
121A	08:38 - 09:19	L.S.	9	Flood
121B	14:40 - 15:09	L.S.	7	Ebb
123A	10:04 - 10:19	M - L.S.	4	Flood
123B	13:08 - 13:25	V.S.	4	Flood
123C	15:03 - 15:17	V.S.	5	Ebb
125A	11:01 - 11:14	V.S.	5	Flood
125B	17:29 - 17:43	F - V.S.	< 3	Ebb
127A	09:19 - 09:44	L.S.	6	Flood
127B	14:07 - 14:30	V.S.	5	Flood
130	11:44 - 12:00	F - L.S.	4 - 7	Ebb
132	11:19 - 11:38	F	3	Ebb
134	16:44 - 17:00	F	3	Ebb
135	00:16 - 00:38	F	< 3	Flood

V.S. = Vertically Stratified   M = Well-mixed condition
L.S. = Longitudinally Stratified   F = Frontal structure evident

The efficiency of the energy transfer process depends on the wind strength, the stability of the atmospheric boundary layer over the water surface, and the basin geometry relative to the wind direction. Of these influences, the wind speed is the dominant factor that determines the actual stress exerted on the water surface, and the response of the wind mixed-layer is a function of this kinematic shear stress.

Wave Actions

A Draper-Tucker wave analysis was performed to extract significant wave heights and periods from the data collected by the two Marine and Harbours wave recording instruments. The surface buoy, which was mounted outside the harbour in 8 m of water, measured an average significant wave height of 0.71 m and a mean period of 7.29 s. The bottom-mounted pressure transducer inside the harbour recorded an average significant wave height of 0.11 m and a 39.52 s mean period. The difference between the larger waves outside the harbour and the smaller waves inside is a measure of the protection provided by the breakwaters. The contribution to flushing by surface wave actions outside Hillarys Boat Harbour was considered to be negligible; however, the surface wave actions within the harbour were important for mixing.
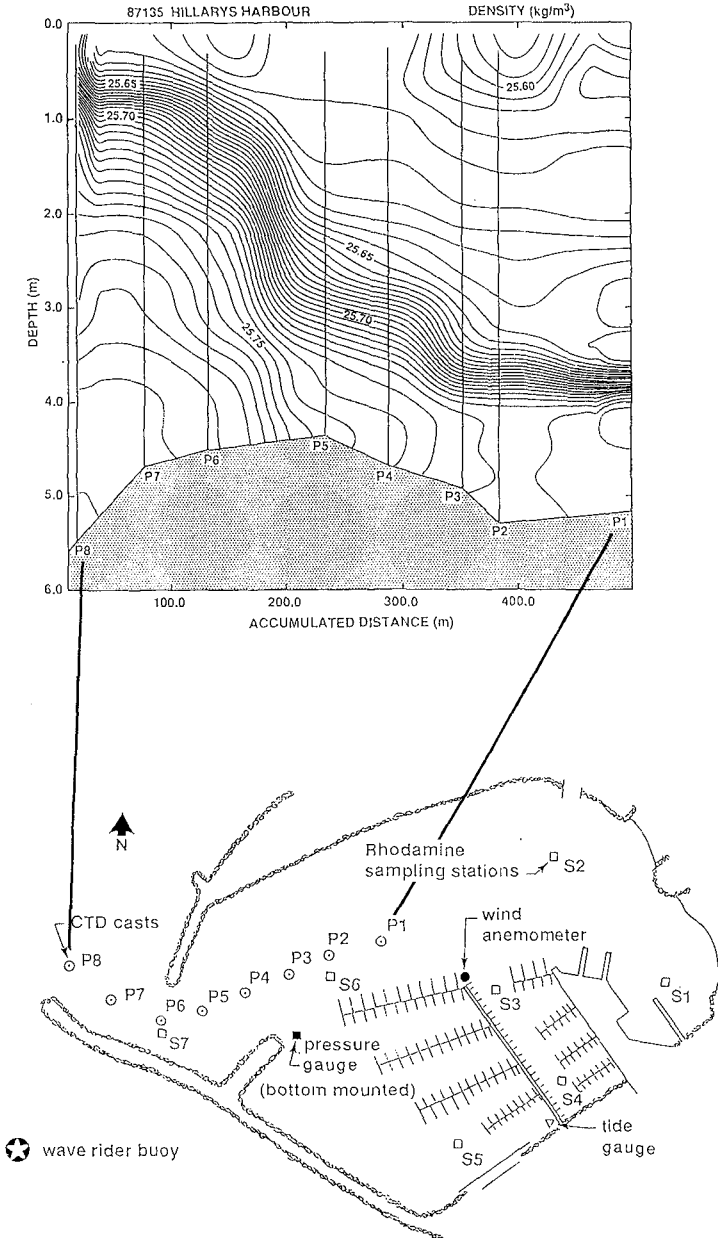
Figure 3 An isopycnal plot derived from 8 CTD casts (P1-P8) on Julian day 135.

Turbulent Mixing

It was necessary to assess the efficiency of turbulent mixing processes because the effectiveness of tidal flushing is dependent on the rate at which the tidal inflow is mixed with the harbour water. The transport of mass by turbulent motions is a function of the kinematic viscosity and the supply rate of kinetic energy. Energy enters a water body at large scales of motion which correspond to the basin dimensions, and it is transferred to smaller scales of motion by random velocity fluctuations and turbulent diffusion. In his universal equilibrium theory, Kolmogorov (1941a,b) formulated the following expression for the smallest length scale which is characteristic of turbulent motion,

$$\eta = (\varepsilon^{-1} \nu^3)^{1/4} \tag{3}$$

where ε is the turbulent kinetic energy dissipation rate and ν is the kinematic viscosity. Typically, η is on the order of a few millimeters. At this level, viscosity becomes important and kinetic energy is dissipated into heat by internal friction forces. From knowing the rate at which kinetic energy is dissipated, the transport rate associated with the turbulent motions can be determined.

An estimate of the turbulent kinetic energy dissipation rate can be determined either directly from measurements of the velocity-shear spectrum, or indirectly from fine-scale temperature gradient measurements (Dillon and Caldwell 1980, and Oakey 1982). The current study made use of the latter approach, which is based on the premise that the spectrum of small-scale temperature variations is related to the energy spectrum by the same wavenumber. Batchelor (1959) used Kolmogorov's (1941) hypothesis to predict the existence of a length scale beyond which no further refinement of the temperature distribution can occur. The smallest length scale for temperature fluctuations is derived by balancing heat advection with thermal diffusion and is known as the Batchelor length scale. The reciprocal of the Batchelor length scale is the Batchelor wavenumber κ_B written as

$$\kappa_B = (\varepsilon \nu^{-1} D^{-2})^{1/4} \tag{4}$$

where D is the molecular diffusivity of heat. Gibson and Schwarz (1963) used Batchelor's results to derive the one-dimensional Batchelor wavenumber spectrum whose upper limit represents the onset of viscous or diffusive effects. Thus, equation (4) can be solved to give an estimate of the turbulent kinetic energy dissipation rate after the maximum Batchelor wavenumber has been identified.

To identify the maximum Batchelor wavenumber, a Wigner-Ville distribution was applied to the microstructure temperature gradient signal from the vertically rising microstructure profiler (RMP) instrument in accordance with the method described in Imberger and Boashash (1986). The Wigner-Ville transform method is an analysis technique whereby the energy content of a non-stationary signal, such as the microstructure temperature gradient, is distributed in a time-frequency domain. This technique yields the instantaneous and maximum frequencies of the energy spectrum. The maximum temperature fluctuation frequency is then converted by a dispersion relationship into a wavenumber representing the maximum Batchelor wavenumber.

The RMP probe was only used on Julian day 119 at two different locations within the harbour. The probe was deployed three times at each location to increase statistical

confidence in the collected data trends. The respective dissipation rates calculated from the temperature measurements are listed in Table 2 along with the corresponding times of deployment and wind speeds.

Table 2 Dissipation rate estimates from RMP temperature measurements.

Julian Day	Time	U_3 (ms^{-1})	ϵ (m^2 s^{-3})
119A$_1$	10:31	2.3	3.1 x 10^{-7}
119A$_2$	10:41	2.3	4.4 x 10^{-7}
119A$_3$	10:48	2.6	4.2 x 10^{-7}
119B$_1$	12:08	3.1	3.8 x 10^{-7}
119B$_2$	12:16	2.3	3.0 x 10^{-7}
119B$_3$	12:30	3.0	3.7 x 10^{-7}

Scaling arguments were used to estimate a time scale for the turbulent diffusion process. The time scale associated with horizontal transport due to turbulent motions can be written as

$$T_x \sim (L_x)^2 / K_x \qquad (5)$$

where K_x is a horizontal diffusion coefficient which represents the non-advective mixing processes; therefore, its real value is highly dependent on the magnitude of these non-linear processes. Fischer et al. (1979) depicted a unified diagram of patch diffusion (after Okubo, 1974) from which it is possible to estimate a diffusion coefficient given the size of a tracer cloud. Given that the width of the harbour is of order 1 x 10^4 cm, K_x was found to have a value of 1 x 10^2 cm^2 s^{-1}. Evaluating (5) with K_x = 1 x 10^{-2} m^{2}s^{-1} and L_x = 100 m gives a value for a horizontal transport time scale of order 10 days, which was representative of the turbulent diffusion processes associated with wind speeds of about 2.5 ms^{-1}. However, it was shown that the harbour remained stratified when wind speeds were less than 3 ms^{-1}, and a baroclinic exchange existed under these conditions. Therefore, it was desirable to know the horizontal transport time scale for the diffusion mechanism under more turbulent conditions than those measured on Julian day 119.

A relationship between the dissipation rate of mechanical energy in the surface mixed-layer and the energy flux from the atmosphere was reported by Oakey and Elliott (1982). They recorded turbulence levels under a variety of wind-wave conditions at a site near Emerald Basin on the Scotian shelf. The correlation between their dissipation and atmospheric forcing data showed a linear relationship between ϵ_I and $(U_{10})^3$. Here, ϵ_I is an average value of the dissipation rate integrated over depth, and U_{10} is an average wind speed measured at 10 m above the water surface for the hour prior to the dissipation measurements.

For the data presented in Table 2, ϵ_I was equal to about 6 x 10^{-6} m^{3}s^{-3} and U_{10} cubed was equal to approximately 30 m^{3}s^{-3}. There was good agreement between these data and those presented by Oakey and Elliott (1982). It was therefore reasonable to assume that the dissipation rate in Hillarys Boat Harbour goes as the 10 m wind speed cubed. Given

that ε goes as $(U_{10})^3$, then doubling the wind speed halves the horizontal transport time scale associated with the diffusive mechanism. Thus, a wind speed equal to 6 ms^{-1} could introduce enough TKE for eddy-diffusion processes to disperse a tracer cloud the size of the harbour in a time of order 5 days. Since the time for dispersion by turbulent motions was greater than the diurnal period of the tide, this indicated that the contribution to flushing by barotropic forcing was limited by mixing and not the size of the tidal prism. Therefore, the 11 day flushing time derived from the tidal prism method was an optimal estimate, which means the actual barotropic flushing time was probably several days longer.

4.0 Discussion of Results

The interpretation of the processed data was simplified by viewing Hillarys Boat Harbour as a small estuary. A partially stratified estuary was defined by Imberger (1976) as "one which possesses a quite definite longitudinal salinity gradient from the mouth to the head of the estuary, but only a very weak vertical or transverse salinity structure". Such a stratification condition requires a fresh water source near the head of the estuary and a vertical mixing mechanism which will overcome the vertical stratification caused by the fresh water input.

It was shown that wind generated turbulence in Hillarys Boat Harbour was sufficient to break down the vertical structure caused by the groundwater seepage, thereby establishing a longitudinal density gradient. Such a density gradient causes a pressure gradient force which is directed from the mouth towards the head of the estuary. A second pressure gradient force results from a surface slope and is generally directed towards the mouth of the estuary. Consequently, a net circulation is established in which a barotropic force due to a surface slope drives a seaward flow in the upper layer, and a baroclinic force caused by a longitudinal density gradient drives a landward flow in the lower layer.

Two-Layer Flow

The concept of critical flow in a two-layer system was first studied by Stommel and Farmer (1952, 1953). They showed that the discharge at the mouth of an estuary can be limited by an interfacial Froude number F_i equal to unity. The interfacial Froude number was defined as

$$F_i = v_1 / (g' \, y_1)^{1/2} \tag{6}$$

where the subscript 1 refers to the upper layer. Critical flow occurs in the upper layer maintaining a critical depth so that the compensating inflow in the lower layer is restricted. Wood (1968) discovered that there are actually two points of control, one at the narrowest section and another at a neighbouring upstream location. The latter control point is called the virtual point of control, and its position is determined by the barotropic flow. The results by Wood (1968) were extended by Armi (1986), who parameterized the flows in terms of the internal Froude numbers in each layer and presented solutions to the non-dimensional continuity and energy equations in a Froude number plane. This approach parallels the specific energy method in that the conditions for critical flow in a two-layer system can be determined from a Froude number diagram just as unstratified critical flow conditions are determined from a specific energy diagram.

For a two-layer flow through a contraction, the non-dimensional continuity equation can
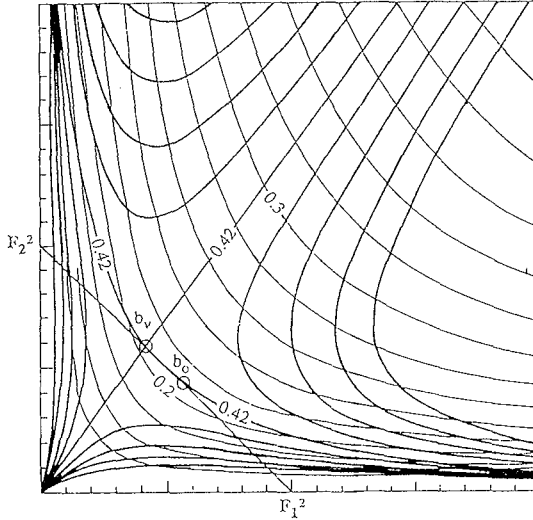
Figure 4   Critical flow conditions on Julian day 135 with $Q_r = 1.4$.

be written as

$$Q_r^{2/3} F_1^{-2/3} + F_2^{-2/3} = (Q_2' / b')^{-2/3} \qquad (7)$$

where Q_2' is the non-dimensional lower layer discharge, b' is the width and $Q_r = Q_1 / Q_2$. The solutions to equation **XX** define the locus of possible Froude number pairs for any given Q_r and Q_2'/b'. For two-layer flow through a contraction, the non-dimensional energy equation in Froude number space is given by Armi (1986) as

$$\Delta H' = \frac{F_2^{-2/3}(1 + 0.5 F_2^2) - 0.5 Q_r^{2/3} F_1^{-2/3} F_1^2}{Q_r^{2/3} F_1^{-2/3} + F_2^{-2/3}} \qquad (8)$$

where $\Delta H'$ is the dimensionless energy difference between the two layers. For small internal Froude numbers, $\Delta H'$ is the same as y_2' measured at the narrowest section. Armi and Farmer (1986) described all the flow properties for maximal two-layer exchange using nine dimensionless equations, nine unknowns and a non-dimensional barotropic flow.

The aforementioned method was applied to Hillarys Boat Harbour using data from Julian day 135 measurements. The barotropic flow for this case was calculated to be 2.85 $m^3 s^{-1}$. Dividing this value by $(g')^{1/2} b_0 (y_1 + y_2)_0^{3/2}$, where $g' = 0.0014 \, ms^{-2}$, $b_0 = 90$ m, and $(y_1 + y_2)_0 = 5$ m, yielded a non-dimensional barotropic flow component $U_0' \approx$ 0.09. This was used to solve for $y_{2'0} \approx 0.42$, $b_v' \approx 1.05$, $Q_1' \approx 0.30$, $Q_2' \approx 0.21$, $v_1' \approx$ 0.56, and $v_2' \approx 0.44$. The subscripts $_0$ and $_v$ refer to the narrowest section and location of the virtual control, respectively. The results are schematically shown in Froude number space in Figure 4. The line connecting (1,0) with (0,1) represents the locus of composite Froude numbers $(G^2 = F_1^2 + F_2^2 = 1)$ that separate subcritical flow $(G^2 < 1)$ from supercritical flow $(G^2 > 1)$. On Julian day 135, a composite Froude number $G^2 = 0.64 + 0.40 = 1.04$ identified the existence of internal critical flow conditions with a normal control at $b_0 = 90$ m and a virtual control at 94.5 m.

Flushing

The tidal prism method was used to calculate an optimal tidal flushing time on the order of 11 days. By superimposing the tidal prism decay rate onto the measured decay rate, it became apparent that at times the Rhodamine WT concentration was dropping at a rate similar to the tidal flushing rate; while at other times, the tracer concentration decayed much faster. This can be seen in Figure 2. An explanation for the variable flushing rate is that a baroclinic flushing mechanism was dominant during calm weather conditions, and the barotropic tide coupled with diffusion processes were responsible for flushing during active mixing periods. A similar case study was reported by Bienfang (1980) in which continual groundwater infiltration produced harbour flushing rates six to ten times those calculated for tidal flushing alone.

The flushing rate due to an internal flow driven by a density variation within Hillarys Boat Harbour was determined using $v_1'_0$ & $v_2'_0$ from Julian day 135. It was shown that $v_1' \approx$ 0.56, and $v_2' \approx 0.44$. Dividing $v_1'_0$ & $v_2'_0$ by $[g'(y_1+y_2)]^{1/2}$ gives their dimensional form as an outflowing upper layer velocity $v_{1_0} \approx 0.045$ ms^{-1}, and an inflowing lower layer velocity $v_{2_0} \approx 0.035$ ms^{-1}. These values appeared to be consistent with drogue measurements conducted on Julian day 119. Defining the smaller of the two velocities as the baroclinic exchange rate, the time required for an uninterrupted baroclinic exchange flow to renew the 1.3 x 10^6 m^3 harbour volume was calculated to be on the order of 2 days! However, it was shown that wind stirring was capable of destroying the vertical stratification, thereby inhibiting the flushing effectiveness of an established baroclinic circulation. Since the total flushing time and the barotropic component were known, it was possible to estimate the percentage of time for which a baroclinic circulation was active.

Substituting a measured total flushing time T_f = 5 days, a barotropic component of 11 days, and a baroclinic flushing time of 2 days into the expression

$$ 1/T_f = 1/T_{Tide+Diffusion} + X/T_{Baroclinic} \qquad (9) $$

indicates that the baroclinic flushing mechanism was active during approximately 20% of the experimental period. It should be remembered that the barotropic flushing time used to solve equation (9) was an optimal estimate. Therefore, the baroclinic flushing process was probably active for a bit more than 20% of the time during the experiment.

5.0   Conclusions

The primary conclusion of this investigation is that within Hillarys Boat Harbour a baroclinic circulation caused by a fresh groundwater influx enhances the barotropic flushing. An overall flushing time of 5 days was measured during the experimental programme, and an optimal tidal flushing time of 11 days was calculated using the tidal prism method. The discrepancy was too large to be explained by experimental error, which meant that another process was accelerating the ongoing tidal exchange flow.

Fine-scale salinity and temperature measurements revealed a range of stratification conditions within the harbour due submarine groundwater discharges. When a vertical stratification condition existed, an internal two-layer flow was established. This flow was shown to be critical near the harbour entrance, which acted as a control on the

depth-discharge relationship. An uninterrupted flushing rate for the observed baroclinic exchange was calculated to be on the order of 2 days. However, a variable wind field was shown to be capable of destroying the gravitational circulation. As a result, the gravitational circulation was estimated to have been active during at least 20% of the experimental period, which was sufficient to cause a two-fold improvement over the tidal flushing time.

Acknowledgment

The Hillarys Boat Harbour flushing study was conducted by the Centre for Water Research, University of Western Australia on behalf of the Department of Marine and Harbours of Western Australia. The writers are grateful to the members of these two organizations for their financial support and cooperative assistance. The authors would also like to thank Dr. L. Armi for suggesting the baroclinic flushing as a possibly important mechanism.

References

Armi, L. (1986) "The Hydraulics of Two Flowing Layers with Different Densities".
    J. Fluid Mech. **163**:27-58.

Armi, L. and Farmer, D. M. (1986)
    "Maximal Two-Layer Exchange Through a Contraction with Barotropic Net Flow.
    J. Fluid Mech. **164**:27-51.

Batchelor, G.K. (1959) "Small Scale Variation of Convected Quantities Like Temperature
    in Turbulent Fluid". J. Fluid Mech. **5**:113-133.

Bienfang, P. (1980) "Water Quality Characteristics of Honokohau Harbor: A Subtropical
    Embayment Affected by Groundwater Intrusion". Pacific Science, 34:279-291.

Carter, G. D. and Imberger, J. (1986) "Vertically Rising Microstructure Profiler".
    J. Atmospheric and Oceanic Tech. 3:462-471.

Dillon, T. M. and Caldwell, D. R. (1980) "The Batchelor Spectrum and Dissipation in the
    Upper Ocean". J. Geophys. Res. **85**:1910-1916.

Dyer, K. R. (1973) *Estuaries: A Physical Introduction.* John Wiley & Sons, pp. 133.

Fischer H. B., List E. J., Koh R. C., Imberger J. and Brooks N. H. (1979)
    Mixing in Inland and Coastal Waters. Academic Press, New York.

Fozdar, F. M. (1983) "Mixed Layer Probe Technical Report".
    Env. Dyn. Ref. ED-83-039, Univ. of Westn. Aust., 68 p.

Fozdar F. M., Parker G. J., and Imberger J. (1985) "Matching Temperature and
    Conductivity Response Characteristics". Amer. Meteor. Soc. pp. 1557-1569.

Gibson, C.H. and Schwarz W.H. (1963) "The Universal Equilibrium Spectra of
    Turbulent Velocity and Scalar Fields". J. Fluid Mech. **16**:365-384.

Imberger, J. (1976) "Dynamics of a Longitudinally Stratified Estuary".
    Proc. 15th Coastal Eng. Conf. pp. 3108-3123.

Imberger, J. (1985) "The Diurnal Mixed Layer". Limnological Oceanogr. **30**:737-488.

Imberger, J. and Berman T. (1986) "An Optimized Pumping System for Vertical Profiling in Aquatic Environments". Env. Dyn. Ref. EFM-1, Univ. of Westn. Aust.

Imberger, J. and Boashash, B. (1986) "Application of the Wigner-Ville Distribution to Temperature Gradient Microstructure: A New Technique to Study Small-Scale Variations". J. Phys. Oceanography. 16:1997-2012.

Johannes, R. E. (1980) "The Ecological Significance of the Submarine Discharge of Groundwater". Marine Ecology Progress Series. 3:365-373.

Kolmogorov, A. N. (1941a) "The Local Structure of Turbulence in an Incompressible Viscous Fluid for very Large Reynolds Numbers". C.R. *Acad. Sci.,* URSS, 30: 301.

Kolmogorov, A. N. (1941b) "Dissipation of Energy in Locally Isotropic Turbulence". C.R. *Acad. Sci.,* URSS, 32: 16.

Nece, N. E. (1984) "Planform Effects on Tidal Flushing of Marinas". J. Waterway, Port, Coastal and Ocean Eng. Div., A.S.C.E., pp.251-269.

Oakey, N. S. (1982) "Determination of the Rate of Dissipation Turbulent Energy from Simultaneous Temperature and Velocity Shear Microstructure Measurements". J. Phys. Oceanography, 12:256-271.

Oakey, N. S. and Elliott, J. A. (1982) "Dissipation Within The Surface Mixed Layer". J. Phys. Oceanography, 12:171-185.

Okubo, A. (1974) "Some Speculations on Oceanic Diffusion Diagrams". Rapp. P. Reun. Cons. Int. Explor. Mer. 167:77-85.

Simpson, J. H. and Nunes, R. A. (1981) "The Tidal Intrusion Front: An Estuarine Convergence Zone". Estuarine and Coastal Shelf Science. 13:257-266.

Smart, P.L. and Laidlaw, I.M.S. (1977) "An Evaluation of Some Fluorescent Dyes for Water Tracing". Water Resources Research. 13:15-33.

Stommel, H and Farmer, H. G. (1952) "Abrupt Change in Width in Two-Layer Open Channel Flow". J. Mar. Res. 11(2):205-214.

Stommel, H and Farmer, H. G. (1953) "Control of Salinity in an Estuary by a Transition". J. Mar. Res. 12:13-20.

UNESCO (1981) "The Practical Salinity Scale 1978, and the International Equation of State 1980". Tenth rep. of the joint panel on oceanographic tables and standards. UNESCO Tech paper in Mar. Sci. 36:13-21.

Wood, I. R. (1968) "Selective Withdrawal from a Stably Stratified Fluid". J. Fluid Mech. 32:209-223.